# Influence of Temporal Interference Stimulation Parameters on Point Neuron Excitability

Tom Plovie, Ruben Schoeters, Thomas Tarnaud, Luc Martens, Wout Joseph, Emmeric Tanghe

***Abstract*— Temporal interference (TI) stimulation is a technique in which two high frequency sinusoidal electric fields, oscillating at a slightly different frequency are sent into the brain. The goal is to achieve stimulation at the place where both fields interfere. This study uses a simplified version of the Hodgkin-Huxley model to analyse the different parameters of the TI-waveform and how the neuron reacts to this waveform. In this manner, the underlying mechanism of the reaction of the neuron to a TI-signal is investigated.**

***Clinical relevance*— This study shows the importance of the parameter choice of the temporal interference waveform and provides insights into the underlying mechanism of the neuronal response to a beating sine for the application of temporal interference stimulation.**

## I. INTRODUCTION

For many years now, deep brain stimulation (DBS) is commonly used as a therapy for refractory Parkinson's Disease [1]. The biggest issue with this treatment is the invasiveness and the possible complications accompanied with it. In [2], a non-invasive variant is proposed to the conventional DBS-method that is used today. This variant is called temporal interference (TI) DBS. Here, (at least) two electrode pairs are placed on top of the scalp. Both electrode pairs create a high frequency oscillating electric field. Moreover, they oscillate at a slightly different frequency resulting in a TI-signal. The key is that experiments on mice showed that the neurons respond to the TI-signal but not to the sinusoids seperately. Because of this, the stimulation focus is more or less restricted to the zone where the two sinusoidal signals interfere [2], [3]. In [2] and [3], it is observed that the neurons respond at the beat frequency ($f_b$) of the TI-signal. The beat frequency is the frequency at which the envelope of the TI-signal repeats itself. Other work was reported where eye movements were regulated to the beat frequency of the TI-signal [4]. However, the beat frequency does not seem to have an influence on the threshold of the input, in contrast to the carrier frequency ($f_c$) [2], [5].

No experiments on humans have done been yet. In order to get more insight in the electric field distribution of TI-DBS in a human brain, finite element simulations have been done [6], [7]. These showed that the positioning of the electrodes and the input intensity are important parameters to specify the stimulation focus. The relevance of this technique was shown because the stimulation site deep in the brain can be more focal than in regular techniques as transcranial alternating current stimulation and transcranial direct current stimulation [6], [7]. The underlying mechanism of the neuronal response to TI-stimulation is largely unknown. Previous studies on this subject have shown that the Fitzhugh-Nagumo, Hodgkin-Huxley (HH) and some mammalian neuron models show correspondence with the experimental results that a neuron is stimulated by the TI-signal and not by the sinusoidal signals [8], [9]. This is not the case for integrate-and-fire neurons, except for when they are put in a neuronal network and slow $\mathrm{GABA_b}$ synapses are included [10].

Because of the non-linear nature of the HH-model, it is a complex model to analyse. Therefore, instead of the HH model, a simplified version of the HH model is used to study the underlying mechanism of TI-stimulation. The mechanism is studied based on the input parameters of the TI-signal. These parameters are the input amplitude and the frequencies of both electric fields.

## II. METHODS

### A. Neuron model

In this study, a simplified version of the Hodgkin-Huxley model is used. The HH-model contains four variables defining the state of the neuron, namely, $V$, $m$, $h$ and $n$. $V$ is the membrane potential. $m$, $h$ and $n$ are the open probabilities of the ion gates. The model can be simplified by reducing number of variables to two. The first simplification is that the m-gate responds infinitely fast and thus $m = m_\infty(V)$, where $m_\infty(V)$ is the steady state value of the m-gate. This can be substantiated because the m-gate generally responds much faster than the h- and n-gate. The second simplification is that $n = 1 - h$. Because the time constants of the h- and n-gate are of the same order of magnitude and the nature of their steady state characteristic, this approximation can be justified. The model is then described by (1) and (2).

$$C_M \frac{dV}{dt} = I_e - (I_L + I_{Na} + I_K) \tag{1}$$

$$\frac{dh}{dt} = \alpha_h(V)(1-h) - \beta_h(V)h \tag{2}$$

with $I_\mathrm{L} = g_L(V - E_L)$, $I_\mathrm{Na} = m_\infty(V)^3 h \overline{g}_{Na}(V - E_{Na})$ and $I_\mathrm{K} = (1-h)^4 \overline{g}_K(V - E_K)$.

Here, $C_M$ is the membrane capacitance, $I_e$ is the input current, $g_L$ is the leak conductance, $\overline{g}_{Na}$ is the maximal

This research was funded by the FWO-project G019121N. T Tarnaud is a postdoctoral Fellow of the FWO-V (Research Foundation Flanders, Belgium). R Schoeters is a PhD Fellow of the FWO-V (Research Foundation Flanders, Belgium).

T. Plovie, R. Schoeters, T. Tarnaud, L. Martens, W. Joseph, E. Tanghe are with the Department of Information Technology (INTEC-WAVES/IMEC), Ghent University/IMEC, Technologypark 126, 9052 Zwijnaarde, Belgium. E-mail: tom.plovie@ugent.be

sodium conductance, $\overline{g}_K$ is the maximal potassium conductance, $E_L$ is the reversal potential of the leak current, $E_{Na}$ is the Nernst potential of sodium and $E_K$ is the Nernst potential of potassium. $\alpha_h(V)$ and $\beta_h(V)$ are the open en closing rates of the h-gate, respectively. Their values are given in [11]. The simulation of this was performed in MATLAB 2021b, using the fixed step Runge-Kutta ode4 solver [12].

### B. Input

The TI-waveform and sinusoidal waveform can be modeled through the input current $I_e$, which is included in (1). Mathematically, the TI-input is then modeled as $I_e = \frac{I_A}{2}(\sin(2\pi f_1 t) + \sin(2\pi f_2 t))$. Here, $I_A$ is the input amplitude, $f_1$ and $f_2$ are the frequencies of the seperate sinusoids constituting the TI-signal and $t$ is the time variable. The carrier frequency and the beat frequency of the TI-signals then become $f_c = \frac{f_1+f_2}{2}$ and $f_b = |f_1 - f_2|$, respectively.

### C. Analysis

*1) Firing rate:* This metric reflects the frequency at which a neuron spikes. An action potential (AP) in this model is defined as the membrane potential exceeding $10$ mV. The firing rate (FR) is then defined by

$$\mathrm{FR} = \frac{n_{AP}}{t_{stim}} \tag{3}$$

where $n_{AP}$ is the number of APs during the stimulation and $t_{stim}$ is the stimulation duration.

*2) Phase diagrams:* Because the model consists of two variables defining the state of the neuron ($V$ and $h$), the neuronal response can be presented in the ($V$, $h$)-plane. This is called the phase diagram. The framework of a phase diagram consists of the $V$-nullcline, $h$-nullcline and a vector field. The $V$-nullcline is the line in the ($V$, $h$)-plane where $\frac{dV}{dt} = 0$ in (1). The $V$-nullcline has to be calculated numerically. The $h$-nullcline is the line in the ($h$, $V$)-plane where $\frac{dh}{dt} = 0$ in (2). The analytical expression of the $h$-nullcline is $h = h_\infty(V)$. The vector field represents the ($dV$, $dh$)-vector for every ($V$, $h$)-combination.

## III. Results

### A. Analyses of phase diagrams

First, it is interesting to get some insight into the framework of the phase diagrams that consists of the $V$-nullcline, $h$-nullcline and the vector field. This framework is shown in Fig. 1. Note that both the $h$-nullcline and $dh$ do not depend on the input current. The input current can thus not influence the y-component of the vector field in the phase diagram. The model has a stable point at the junction of both nullclines. When the input current is $0$ $\frac{\mu\mathrm{A}}{\mathrm{cm}^2}$, the stable point is at ($V = -72$ mV, $h = 0.665$). For an input current of $-105$ $\frac{\mu\mathrm{A}}{\mathrm{cm}^2}$ (minimal input current of all simulations depicted in this paper), there is no stable point in the scope of realistic values for the membrane potential. For a constant input current of $105$ $\frac{\mu\mathrm{A}}{\mathrm{cm}^2}$ (maximal input current of all simulations depicted in this paper), the stable point is at ($V = -63.2$ mV, $h = 0.36$). It can be seen that the $V$-nullcline can take on two different shapes. It can either be the shape of the black line in Fig. 1a where there is a jump from $-\infty$ to $+\infty$ and a local minimum or the shape of the black line in Fig. 1b, where the $V$-nullcline reaches a local minimum and maximum. The first case is found for $I_A < -7$ $\frac{\mu\mathrm{A}}{\mathrm{cm}^2}$ and the second case for $I_A > -7$ $\frac{\mu\mathrm{A}}{\mathrm{cm}^2}$.

### B. Influence of the beat frequency

Fig. 2a and 2b show the phase diagrams for different beat frequencies of the TI-input. It can be seen that with a beat frequency of $30$ Hz, only one AP is elicited, i.e., at the stimulation onset. For a beat frequency of $50$ Hz , the firing rate is $50$ Hz. Every beat can thus elicit an AP. For the TI-signal with a beat frequency of $100$ Hz, the firing rate is still $50$ Hz. So the neuron only fires every other beat. It stands out that for the beat frequency of $50$ Hz, the node of the TI-signal is very close to the stable point of the neuron. The node is reached around $h = 0.620$. For the $30$ Hz case, the envelope is still decreasing in amplitude at that point. For the input of $100$ Hz, $h$ has a value of $0.411$ in the first node after firing of the AP.

When the state of the neuron reaches the region around its stable point, it oscillates between $h$-values of $0.62$ and $0.69$ for both the input of $30$ Hz and $50$ Hz. The difference is that the $30$ Hz-signal reaches a maximal membrane potential during these oscillations of only $-63$ mV while the $50$ Hz-signal goes upto $-56$ mV in the last oscillation before the AP. For the $50$ Hz-signal, the neuron spikes with an $h$-value around $0.61$. For the input of $100$ Hz, the $h$-value is around $0.624$ when the neuron spikes. The thresholds for spiking at the beat frequency for the input signals with a beat frequency of 30 Hz, 50 Hz and 100 Hz are $119.75$ $\frac{\mu\mathrm{A}}{\mathrm{cm}^2}$, $98.85$ $\frac{\mu\mathrm{A}}{\mathrm{cm}^2}$ and $190.25$ $\frac{\mu\mathrm{A}}{\mathrm{cm}^2}$, respectively. The most important $h$-values and the threshold values for spiking at the beat frequency are summarized in Table I.

### C. Influence of the carrier frequency

The results for simulations with different carrier frequencies are shown in Fig. 3. It immediately stands out that the oscillations at low membrane potentials after the AP are much bigger for the lowest carrier frequency. The minimal membrane potential is $-91.5$ mV for the signal with a carrier frequency of $1$ kHz and $-87.7$ mV for the signal with a carrier frequency of $2$ kHz. Further on, the maximal $h$-value is higher in the case of a carrier frequency of $2$ kHz. It goes up to $0.667$, while the $h$-value only reaches $0.651$ for the case of a carrier frequency of $1$ kHz. On the other hand, the value of the h-gate at the start of the AP is around $0.600$ for a carrier frequency of $2$ kHz and $0.630$ for a carrier frequency of $1$ kHz. The important $h$-values are again summarized together with the thresholds for spiking at the beat frequency in Table I.

## IV. Discussion

### A. Influence of the beat frequency

For the beat frequency, it was seen that when the beat frequency is too high, some beats do not elicit an AP when

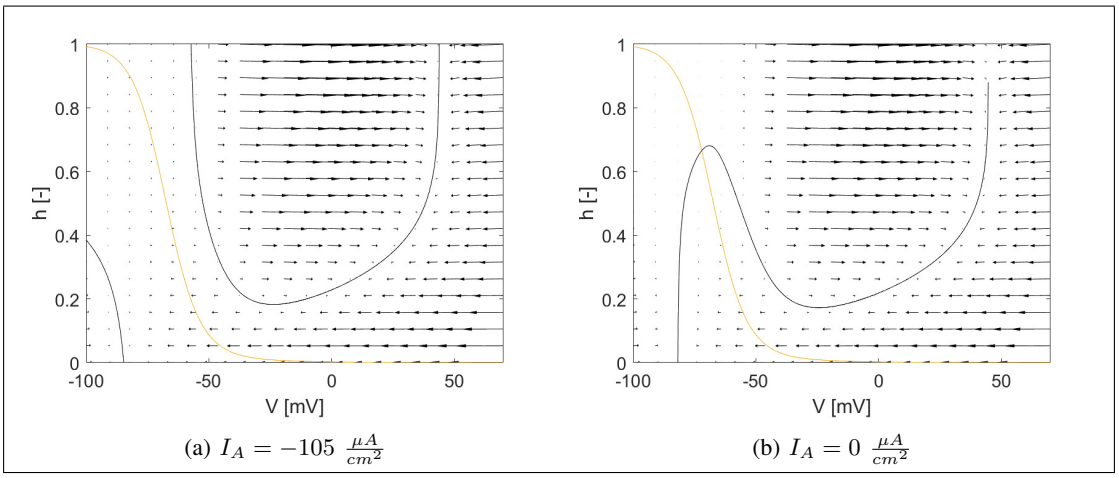


(a) $I_A = -105\ \frac{\mu A}{cm^2}$ (b) $I_A = 0\ \frac{\mu A}{cm^2}$

Fig. 1: Nullclines and vector fields in the phase diagram for different constant input currents $I_A$. Black line: $V$-nullcline. Yellow: $h$-nullcline.

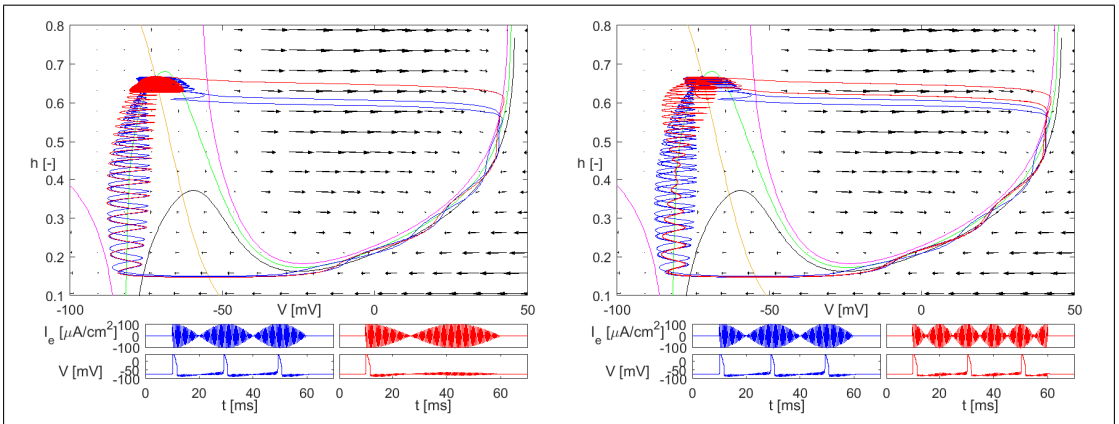


(a) Red: beat frequency of 30 Hz. Blue: beat frequency of 50 Hz.

(b) Red: beat frequency of 100 Hz, Blue: beat frequency of 50 Hz

Fig. 2: Phase diagram and time signals for a stimulation with a TI-signal with an amplitude of 105 $\frac{\mu A}{cm^2}$, a carrier frequency of 2 kHz and different beat frequencies. In the plots as a function of time, $V$ is given in mV and $I_e$ is given is $\frac{\mu A}{cm^2}$. Pink: $V$-nullcline for $I_A = -105\ \frac{\mu A}{cm^2}$. Green: $V$-nullcline for $I_A = 105\ \frac{\mu A}{cm^2}$. Black: $V$-nullcline for $I_A = 0\ \frac{\mu A}{cm^2}$. Yellow: $h$-nullcline. The vector field is shown for $I_A = 0\ \frac{\mu A}{cm^2}$.

the input intensity is too low (see Fig. 2b). This is mainly because the envelope of the TI-signal starts to increase again at a point where the $h$-value is still very low. Because of this, the $h$-value cannot reach a value that is high enough when the TI-signal reaches its maximum. Instead, multiple beats are required in order to initiate a new AP. Consequently, a higher input current is needed to elicit firing at beat frequency. When the beat frequency is lowered (Fig. 2a), the node of the TI-signal is reached at higher $h$-values and the threshold for the input current will decrease.

Another interesting finding is that the $h$-value is lower right before the AP in the case of a beat frequency of 50 Hz compared to a the case of a beat frequency of 100 Hz. The reason for this is that the evelope rises slower. The characteristic of the h-gate is that it decreases with increasing membrane potential. Because of the time constant of the h-gate, there will be a reaction delay to the membrane potential. As the envelope increases faster, the h-gate will decrease less because of this reaction delay. In that case, the AP will be created at a higher $h$-value as seen in the simulation. For a lower beat frequency, the envelope will increase slower and the h-gate will be lower at the start of the AP. However, from the shape of the $V$-nullcline in the case of the black lines of

TABLE I: Summary of important $h$-values in the phase diagram and input thresholds for firing at the beat frequency ($I_{th}$) for different combinations of the beat and carrier frequency. The $h$-values are for an input amplitude of 105 $\frac{\mu A}{cm^2}$

| Beat frequency [Hz] | 30 | 50 | | 100 |
|---|---|---|---|---|
| Carrier frequency [kHz] | 2 | 1 | 2 | 2 |
| Maximal $h$-value [-] | 0.668 | 0.651 | 0.668 | 0.667 |
| $h$-value right before AP [-] | / | 0.630 | 0.600 | 0.624 |
| $I_{\text{th}}$ [$\frac{\mu A}{cm^2}$] | 119.75 | 49.20 | 98.85 | 190.25 |

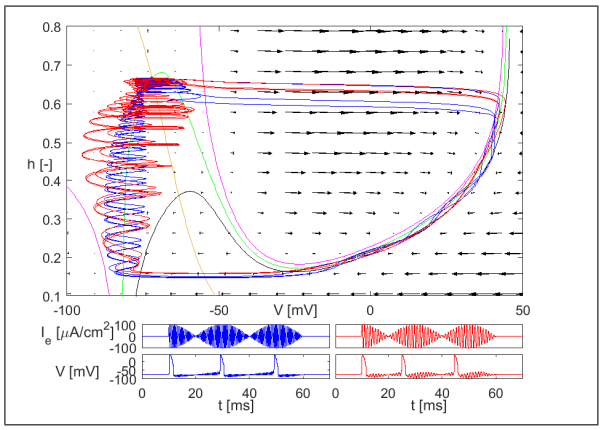


Fig. 3: Phase diagram and time signals for a stimulation with a TI-signal with an amplitude of 105 $\frac{\mu\mathrm{A}}{\mathrm{cm}^2}$ and a beat frequency of 50 Hz. In the plots as a function of time, $V$ is given in $\mathrm{mV}$ and $I_e$ is given is $\frac{\mu\mathrm{A}}{\mathrm{cm}^2}$. Red: carrier frequency of 1 kHz, Blue: carrier frequency of 2 kHz. Other Pink, green, yellow, black and vector field: similar as Fig. 2

Fig. 1a and 1b, it can be deduced that for a lower $h$-value, a higher membrane potential is needed to elicit an AP. In other words, the state of the neuron in the phase diagram should be above the $V$-nullcline for a time that is long enough to shoot to the right of the phase diagram. Because the $h$-value right before an AP is lower for a lower beat frequency, there will be a moment where the h-gate becomes too low for an AP to follow. As a result, the state of the neuron will remain around its stable point of $I_A = 0$ $\frac{\mu\mathrm{A}}{\mathrm{cm}^2}$, as observed for a TI-input with $f_b = 30$ Hz. If you then assume that a single sinusoid is the limit situation of $f_b \to 0$, it is clear that the input threshold to achieve periodic spiking will be lower for a TI-signal with $f_b \neq 0$.

From the above discussion, it could be concluded that there should be a beat frequency where the threshold for the input current is minimal.

### *B. Influence of the carrier frequency*

The main effect of an increasing carrier frequency is that the amplitude of the oscillations of the membrane potential are smaller.It is observed that a higher input intensity is needed to achieve spiking. The reason why the oscillations become smaller is the following. The oscillations of the input current are translated in the phase diagram to a changing $V$-nullcline and a changing vector field. The $V$-nullcline constantly oscillates between the pink and the green outer line while the state of the neuron is attracted to that nullcline in the x-direction. For two input signals with the same amplitude and a different fundamental frequency, the outer lines for the $V$-nullcline will be the same, but the phase diagram will oscillate faster between both outer lines. The speed at which the state of the neuron evolves towards the nullclines, however, will not change. Because of this, the oscillations will be smaller for the signal with a higher carrier frequency resulting in a higher input needed to achieve spiking.

On the other hand it was noticed that the signal with lower carrier frequency has a higher maximal $h$-value, but a lower $h$-value right before the AP. This is mainly because in every oscillation of the carrier frequency the $h$-value decreases, while the envelope of the TI-signal is increasing, as the discussion above. Because the oscillations are bigger along the x-axis for a lower carrier frequency, less oscillations of the carrier frequency are needed to achieve the AP which in this case results in a higher $h$-value. However, because of these larger oscillations of the membrane potential, the state of the neuron reaches different regions in the phase diagram. Because of this it is possible that the optimal beat frequency for temporal interference stimulation is dependent on the carrier frequency.

The results for the influence of the carrier frequency on the threshold to achieve spiking are in line with the experimental results of [2] and [5]. Namely that a higher input is needed for higher carrier frequencies. In contrast, these papers stated that the beat frequency does not have an influence on the input threshold. In our results it was shown that when the beat frequency is too high, not every beat can elicit an AP. On the other hand, when the beat frequency is too low, a higher input is needed to achieve spiking as well. It is possible that the model used in this study lacks complexity to get the same results as in experiments. Additionally, a different definition is used for the threshold which could explain the different results. On the other hand the effect of the beat frequency seems rather small for low beat frequencies. It could thus be possible that noise is involved in the experimental results, so the effect is just too small to see in reality.

## REFERENCES


[1] N. Malek, "Deep Brain Stimulation in Parkinson's Disease," *Neurology India*, vol. 67, no. 4, pp. 968–978, 2019.

[2] N. Grossman *et al.*, "Noninvasive deep brain stimulation via temporally interfering electric fields," *Cell*, vol. 169, pp. 1029–1041.e16, 6 2017.

[3] ——, "Translating temporal interference brain stimulation to treat neurological and psychiatric conditions," *JAMA Neurology*, vol. 75, no. 11, pp. 1307–1308, 2018.

[4] Song *et al.*, "Temporal interference stimulation regulates eye movements and neural activity in the mice superior colliculus," in *2021 43rd Annu. Int. Conf. IEEE Eng. Med. Biol. (EMBC)*, 2021, pp. 6231–6234.

[5] J. Gomez-Tames *et al.*, "Multiscale computational model reveals nerve response in a mouse model for temporal interference brain stimulation," *Frontiers in Neuroscience*, vol. 15, 6 2021.

[6] S. Rampersad *et al.*, "Prospects for transcranial temporal interference stimulation in humans: A computational study," *NeuroImage*, vol. 202, 11 2019.

[7] J. von Conta *et al.*, "Interindividual variability of electric fields during transcranial temporal interference stimulation (ttis)," *Scientific Reports*, vol. 11, 12 2021.

[8] J. Cao and P. Grover, "Do single neuron models exhibit temporal interference stimulation?" *2018 IEEE Biomedical Circuits and Systems Conference (BioCAS)*, pp. 1–4, 2018.

[9] ——, "The mechanics of temporal interference stimulation," *bioRxiv*, 2020.

[10] Z. Esmaeilpour *et al.*, "Temporal interference stimulation targets deep brain regions by modulating neural oscillations," *Brain Stimulation*, vol. 14, no. 1, pp. 55–65, 2021.

[11] A. L. Hodgkin and A. Huxley, "A quantitative description of membrane current and its application to conduction and excitation in nerve," *Journal of Physiology*, vol. 117, no. 1, pp. 500–544, 1952.

[12] Mathworks, "Solver," 2021. [Online]. Available: https://nl.mathworks.com/help/simulink/gui/solver.html